ROCKY MOUNTAIN
JOURNAL OF MATHEMATICS
Volume 48, Number 1, 2018

CONSTRAINED SHAPE PRESERVING RATIONAL CUBIC FRACTAL INTERPOLATION FUNCTIONS

A.K.B. CHAND AND K.R. TYADA

ABSTRACT. In this paper, we discuss the construction of $\mathcal{C}^1$-rational cubic fractal interpolation function (RCFIF) and its application in preserving the constrained nature of a given data set. The $\mathcal{C}^1$-RCFIF is the fractal design of the traditional rational cubic interpolant of the form $p_i(\theta)/q_i(\theta)$, where $p_i(\theta)$ and $q_i(\theta)$ are cubic and quadratic polynomials with three tension parameters. We present the error estimate of the approximation of RCFIF with the original function in $\mathcal{C}^k[x_1, x_n]$, $k = 1, 3$. When the data set is constrained between two piecewise straight lines, we derive the sufficient conditions on the IFS parameters of the RCFIF so that it lies between those two lines. Numerical examples are given to support the theoretical results.

1. Introduction. Visualization of discrete scientific data in a continuous manner plays a significant role in the fields of science and engineering. Data obtained from scientific experiments or complex phenomena are broadly classified as positive, monotone, convex or concave, constrained by curves or surfaces and their combinations based on the values of data according to their graphs. For example, the amounts of products obtained in chemical experiments are positive, the resistivity of metals increases monotonically with increasing temperature, the resistivity of semiconductors decreases monotonically with increasing temperature, path of a projectile with some initial velocity and angle of projection is always concave and amplitude of alternating current

2010 AMS *Mathematics subject classification.* Primary 28A80, 37C25, 41A30, 41A55, 42A15.

Keywords and phrases. Iterated function systems, fractal interpolation, convergence analysis, bounding Cauchy remainder, Peano-kernel theorem, constrained data interpolation, positivity.

This project was supported by the Department of Science & Technology, India, SERCDST Project No. SR/S4/MS:694/10.

Received by the editors on May 7, 2015, and in revised form on October 25, 2016.

DOI:10.1216/RMJ-2018-48-1-75

with respect to time shows convex and concave properties in some particular time period. Splines have proved to be enormously important in smooth curve representations of discrete data in a continuous manner. In the introductory period of spline theory, polynomial splines were extensively studied for different types of shaped data in the literature, see for instance [**3, 9, 20, 32**] and the references therein. Since the classical polynomial spline interpolant representation available in the literature is unique for given data, and it simply depends upon the data points, it is difficult to preserve all of the hidden shape properties of the given data, and consequently, is not suitable for interactive curve/surface design problems. For this reason, a user needs interactive and efficient shape preserving smooth interpolation schemes for a given shaped data. By introducing a shape parameter in each sub-interval, Delbourgo and Gregory [**22**] and Gregory and Sarfraz [**23**] developed shape preserving piecewise rational spline interpolants for local shape modification. Rational splines play an important role in geometric modeling, computer graphics, CAGD and reverse engineering due to the flexibility offered by the shape parameters in each subinterval of the domain function. Using this technique, variants of shape preserving rational interpolants with shape parameters have been developed, see for instance, [**2, 25, 30, 31, 33**] and the references therein.

Although the classical splines, for example polynomial, exponential, rational, B-splines, etc., interpolate data smoothly, certain derivatives of the classical interpolants are either piecewise smooth or globally smooth in nature. Therefore, classical interpolants are not suitable for approximating functions that have an irregular nature or fractality in their first order derivatives. Extremely misguided results, violating the inherited features of the data, can be seen when undesirable oscillations occur, for example, the fall of a spherical ball in a warm micellar solution [**26**], the motion of a pendulum on a cart in an electromechanical system [**16**] and the motion of electrons inside a cyclotron [**24**]. On the other hand, fractal interpolation is an ideal tool in such a scenario as well. In addition to the theoretical interest, fractal interpolants possess fractality (or irregularity) in the functions or their derivatives so that they can very accurately approximate the above types of non-linear phenomena.

Fractal interpolation is a modern and advanced technique for analyzing various scientific data obtained from some complicated unknown

functions and scientific phenomena. Barnsley [**5**] coined the term *fractal interpolation function* (FIF) which was constructed based on the theory of iterated functions system (IFS). An IFS ensures an attractor which is the graph of a continuous function that interpolates the given data points. FIFs are the fixed points of the Read-Bajraktaverić operator [**5, 28**], defined on suitable function spaces. By using FIFs, not only the rough but also the smooth structures may be constructed, whose derivatives have non-integer dimensions [**6, 21, 27**] that vary according to the IFS parameters. Barnsley and Harrington [**8**] introduced the construction of k-times differentiable polynomial spline FIF with a fixed type of boundary condition. The polynomial spline FIFs with general boundary conditions were recently studied in [**10, 12, 14, 29**]. A specific feature of the spline FIF is that its certain derivative can be used to capture the irregularity associated with the original function from where the interpolation data is obtained. Chand and Kapoor [**11**] developed a spline coalescence hidden variable fractal interpolation function whose derivative is a typical fractal function and is a generalization of the hidden variable fractal interpolation function introduced by Barnsley et al. [**7**]. Dalla and Drakopoulos [**17**] introduced polar fractal interpolation functions and developed the range restriction concept for affine FIF.

In this paper, we wish to study the interpolation and approximation of a data generating function for constrained data. Constrained data interpolation has wide applications in real world problems: (i) to eliminate undesigned bumps or wiggles in the prominent lines of the roof of a car; (ii) to eliminate any oscillations which could affect the aerodynamic properties of the resulting surface of network curves consisting of the surface of the tail of an aircraft; (iii) to eliminate high contrast temperature distribution during cold water reignition into a hydro-thermal reservoir; and (iv) to prevent oscillations and overshoot at intermediate points in engineering applications. Abbas [**1**] constructed a $\mathcal{C}^1$-piecewise rational cubic function to preserve the shape of constrained 2D and 3D data. Awang [**4**] developed a $\mathcal{C}^2$-rational cubic function to 2D constrained data interpolation. Duan [**18, 19**] constructed a type of rational spline based upon function values to constrain the interpolating curve between two piecewise straight lines. Hussain et al. [**25, 30, 31, 33**] used different types of $\mathcal{C}^1$-piecewise rational cubic functions to preserve the shape of various constrained

data. Shape preservation of scientific data through different types of smooth rational FIFs was very recently introduced in **[13, 14, 15, 34, 35]**. Motivated by the work of Duan in constrained interpolation, we have proposed the smooth RCFIF such that it can be used for shape preservation. In particular, when the interpolation data set lies in between the two given piecewise straight lines, the IFS parameters of the proposed RCFIF are restricted so that our interpolant lies between those straight lines. Development of RCFIF has many advantageous features such as: it does not require any additional knots and it is useful for the visualization of data with or without slopes at the knots.

The paper is organized as follows. In Section 2, the general theory of FIF for a given data set is reviewed. The construction of $\mathcal{C}^1$-RCFIFs passing through a set of data points is discussed in Section 3. In Section 4, we deduce the error estimation of the RCFIF with an original function for convergence results. In Section 5, the range of scaling factors and shape parameters is restricted according to sufficient conditions so that the developed RCFIF lies between two piecewise straight lines. In Section 6, we address the data locality of the rational fractal interpolation by perturbing the data, followed by conclusions in Section 7.

2. Preliminaries of FIF theory via IFS theory. Let $\mathcal{P} : \{x_1, x_2, \ldots, x_n\}$ be a partition of the real compact interval $I = [x_1, x_n]$, where $x_1 < x_2 < \cdots < x_n$. Denote $\Lambda := \{1, 2, \ldots, n-1\}$ and $\Lambda^* := \{1, 2, \ldots, n\}$. Let a set of data points $\{(x_j, f_j) \in I \times K : \ j \in \Lambda^*\}$ be given, where K is a compact set in $\mathbb{R}$. Let $I_i = [x_i, x_{i+1}]$ and $L_i : I \to I_i, \ i \in \Lambda$, be contractive homeomorphisms such that

$$L_i(x_1) = x_i, \qquad L_i(x_n) = x_{i+1}, \quad i \in \Lambda. \tag{2.1}$$

Let $C = I \times K$, and consider $n-1$ mappings $F_i : C \to K$ which are continuous in the first argument and are contractions in the second argument, satisfying

$$F_i(x_1, f_1) = f_i, \qquad F_i(x_n, f_n) = f_{i+1}, \quad i \in \Lambda. \tag{2.2}$$

Now, define functions

$$\omega_i : C \longrightarrow I_i \times K$$

such that $\omega_i(x, f) = (L_i(x), F_i(x, f))$ for all $i \in \Lambda$. Since ω_i are contractions, the set-valued Hutchinson map

$$W(\cdot) = \bigcup_{i\in\Lambda} \omega_i(\cdot)$$

is a contraction map on the set of non-empty subsets of C. Then, $\{C; \omega_i, i \in \Lambda\}$ is called a *hyperbolic* IFS.

Proposition 2.1 ([**5**]). *The* IFS $\{C; \omega_i, i \in \Lambda\}$ *defined above admits a unique attractor* G *such that* G *is the graph of a continuous function* $g : I \to K$, *which interpolates the data set* $\{(x_j, f_j) \in I \times K : \ j \in \Lambda^*\}$, *i.e.,* $g(x_j) = f_j$ *for* $j \in \Lambda^*$.

The above function g is called an FIF associated with the IFS $\{C; \omega_i(x, f), \ i \in \Lambda\}$. The functional representation of g follows from the fixed point of the Read-Bajraktarević operator T [**28**]. The FIF g satisfies the following functional equation:

$$Tg(x) \equiv F_i(L_i^{-1}(x), g \circ L_i^{-1}(x)) = g(x), \quad x \in I_i, \ i \in \Lambda. \tag{2.3}$$

The standard IFS in the literature of FIF theory is

$$\{C; \omega_i(x, f), \ i \in \Lambda\}, \tag{2.4}$$

where $L_i(x) = a_i x + b_i$, $F_i(x, f) = \alpha_i f + M_i(x)$ with

$$M_i : I \longrightarrow \mathbb{R}$$

suitable continuous functions such that (2.2) is satisfied. The multiplier α_i is called a *scaling factor* of the transformation ω_i, and $\alpha = (\alpha_1, \alpha_2, \ldots, \alpha_{n-1})$ is the scale vector associated with the IFS (2.4). The scaling vector gives an additional degree of freedom to FIFs over their counterparts in classical interpolation and allows for the modification of their shape preserving properties. The existence of a spline FIF was given by Barnsley and Harrington [**8**] based on the calculus of fractal functions, and that result has been extended for the existence of rational spline FIF in the next theorem [**13**].

Theorem 2.2. *Let* $\{(x_j, f_j) : j \in \Lambda^*\}$ *be a given data set such that* $x_1 < x_2 < \cdots < x_n$. *Suppose that* $L_i(x) = a_i x + b_i$, *where* $a_i = (x_{i+1} - x_i)/(x_n - x_1)$, $b_i = (x_n x_i - x_1 x_{i+1})/(x_n - x_1)$ *and* $F_i(x, f) = \alpha_i f + M_i(x)$, $M_i(x) = p_i(x)/q_i(x)$, $p_i(x)$ *and* $q_i(x)$ *are chosen polynomials of degree* r *and* s, *respectively, and* $q_i(x) \neq 0$ *for all* $x \in [x_1, x_n]$

for $i \in \Lambda$. Suppose, for some integer $p \geq 0$, $|\alpha_i| < a_i^p$, $i \in \Lambda$. For $m = 1, 2, \ldots, p$, let

$$
\begin{aligned}
F_{i,m}(x, f) &= \frac{\alpha_i f + M_i^{(m)}(x)}{a_i^m}, \\
f_{1,m} &= \frac{M_1^{(m)}(x_1)}{a_1^m - \alpha_1}, \\
f_{n,m} &= \frac{M_{n-1}^{(m)}(x_n)}{a_{n-1}^m - \alpha_{n-1}},
\end{aligned} \tag{2.5}
$$

where $M_i^{(m)}(x)$ represents the mth derivative of $M_i(x)$. If $F_{i,m}(x_n, f_{n,m}) = F_{i+1,m}(x_1, f_{1,m})$, $i = 1, 2, \ldots, n-2$, $m = 1, 2, \ldots, p$, then the IFS *$\{C; \omega_i(x, f) = (L_i(x), F_i(x, f)),\ i \in \Lambda\}$ determines a rational* FIF *$\Phi \in \mathcal{C}^p[x_1, x_n]$ such that $\Phi(L_i(x)) = \alpha_i \Phi(x) + M_i(x)$, and $\Phi^{(m)}$ is the* FIF *determined by $\{I \times \mathbb{R}; w_{i,m}(x, f) = (L_i(x), F_{i,m}(x, f)),\ i = 1, \ldots, n-1\}$ for $m = 1, 2, \ldots, p$.*

3. $\mathcal{C}^1$-rational cubic fractal interpolation function. In this section, we construct the RCFIF with three shape parameters in each subinterval with the aid of Theorem 2.2. Let $\{(x_j, f_j),\ j \in \Lambda^*\}$ be a given set of interpolation data for an original function Ψ such that $x_1 < x_2 < \cdots < x_n$. Consider the IFS

$$\{I \times K; \omega_i(x, f) = (L_i(x), F_i(x, f)),\ i \in \Lambda\},$$

where $L_i(x) = a_i x + b_i$ and $F_i(x, f) = \alpha_i f(x) + M_i(x)$, $M_i(x) = p_i(x)/q_i(x)$, $p_i(x)$ and $q_i(x)$ are cubic polynomials, $q_i(x) \neq 0$ for all $x \in [x_1, x_n]$ and $|\alpha_i| < a_i$, $i \in \Lambda$. Let

$$F_i^{(1)}(x, d) = \frac{\alpha_i d + M_i^{(1)}(x)}{a_i},$$

where $M_i^{(1)}(x)$ is the first order derivative of $M_i(x)$, $x \in [x_1, x_n]$. $F_i(x, f)$ satisfies the following join up conditions:

$$
\begin{aligned}
F_i(x_1, f_1) &= f_i, \qquad F_i(x_n, f_n) = f_{i+1}, \\
F_i^{(1)}(x_1, d_1) &= d_i, \qquad F_i^{(1)}(x_n, d_n) = d_{i+1},
\end{aligned} \tag{3.1}
$$

where d_i denotes the first order derivative of Ψ with respect to x at knot x_i. The attractor of the above IFS will be the graph of a $\mathcal{C}^1$-

rational cubic FIF. From (2.3), it may be observed that our FIF can be written as:

$$\Phi(L_i(x)) = \alpha_i \Phi(x) + M_i(x) = \alpha_i \Phi(x) + \frac{p_i(\theta)}{q_i(\theta)}, \tag{3.2}$$

where

$$p_i(\theta) = (1-\theta)^3 A_i + \theta(1-\theta)^2 B_i + \theta^2(1-\theta) C_i + \theta^3 D_i,$$
$$q_i(\theta) = (1-\theta)^2 u_i + \theta(1-\theta) w_i + \theta^2 v_i,$$
$$\theta = \frac{x - x_1}{l}, \quad l = x_n - x_1, \quad x \in I,$$

and u_i, v_i and w_i are positive shaped parameters. In order to ensure that the rational cubic FIF is $\mathcal{C}^1$-continuous, the following interpolation conditions are imposed:

$$\begin{aligned} \Phi(L_i(x_1)) &= f_i, & \Phi(L_i(x_n)) &= f_{i+1}, \\ \Phi'(L_i(x_1)) &= d_i, & \Phi'(L_i(x_n)) &= d_{i+1}. \end{aligned} \tag{3.3}$$

From (3.2) and (3.3), it is clear that, at $x = x_1$, we get

$$\Phi(L_i(x_1)) = f_i \Longrightarrow f_i = \alpha_i f_1 + \frac{A_i}{u_i} \Longrightarrow A_i = u_i(f_i - \alpha_i f_1).$$

Similarly, at $x = x_n$, we obtain

$$\Phi(L_i(x_n)) = f_{i+1} \Longrightarrow f_{i+1} = \alpha_i f_n + \frac{D_i}{v_i} \Longrightarrow D_i = v_i(f_{i+1} - \alpha_i f_n).$$

Taking $x = x_1$ in $\Phi'(L_i(x))$ and using (3.3), we have

$$\begin{aligned} \Phi'(L_i(x_1)) = d_i &\Longrightarrow a_i d_i = \alpha_i d_1 + \frac{u_i(B_i - 3A_i) - A_i(w_i - 2u_i)}{\ell u_i^2} \\ &\Longrightarrow B_i = (u_i + w_i)(f_i - \alpha_i f_1) + \ell u_i(a_i d_i - \alpha_i d_1). \end{aligned}$$

Similarly, computing $\Phi'(L_i(x))$ at $x = x_n$ and using (3.3), we obtain

$$\begin{aligned} \Phi'(L_i(x_n)) = d_{i+1} &\Longrightarrow a_i d_{i+1} = \alpha_i d_n + \frac{v_i(3D_i - C_i) - D_i(2v_i - w_i)}{\ell v_i^2} \\ &\Longrightarrow C_i = (v_i + w_i)(f_{i+1} - \alpha_i f_n) - \ell v_i(a_i d_{i+1} - \alpha_i d_n). \end{aligned}$$

Now substituting A_i, B_i, C_i and D_i in (3.2), we obtain the required $\mathcal{C}^1$-RCFIF with the numerator,

$$\begin{aligned} p_i(\theta) &= u_i(f_i - \alpha_i f_1)(1-\theta)^3 \\ &\quad + \{(u_i + w_i)(f_i - \alpha_i f_1) + \ell u_i(a_i d_i - \alpha_i d_1)\}\theta(1-\theta)^2 \\ &\quad + \{(v_i + w_i)(f_{i+1} - \alpha_i f_n) - \ell v_i(a_i d_{i+1} - \alpha_i d_n)\} \\ &\quad \times \theta^2(1-\theta) + v_i(f_{i+1} - \alpha_i f_n)\theta^3. \end{aligned}$$

In most applications, the derivatives $d_j (j \in \Lambda^*)$ are not given and hence must be calculated either from the given data or by some numerical methods. In this paper, we have calculated d_j, $j \in \Lambda^*$, from the given data using the arithmetic mean method.

Note that an FIF is recursively defined using the implicit functional equation (2.3) and, to obtain the actual interpolant, it is necessary to continue the iterations indefinitely. However, a small number of iterations usually gives sufficiently good approximations.

It is worthwhile mentioning here that points are generated through the maps (L_i, F_i), $i \in \Lambda$. From the given n data points, we introduce new $n-2$ points in each of the $n-1$ subintervals through the maps (L_i, F_i) in the first iteration. Consequently, we have a total of $(n-1)(n-2) + n = (n-1)^2 + 1$ data points at the end of the first iteration. Similarly, we have $(n-1)((n-1)^2 - 1) + n = (n-1)^3 + 1$ points at the end of the second iteration. By induction, it follows that, at the rth iteration, we have values of the FIF g exactly at $(n-1)^{r+1}+1$ distinct points of the interpolation interval; thus, the computation of points is of exponential order and an overall view of the function is quickly obtained.

Remark 3.1. If $\alpha_i = 0$ for all $i \in \Lambda$, the RCFIF Φ becomes the classical rational cubic interpolation function $S(x)$ (say), defined in **[30]**, on each subinterval $[x_i, x_{i+1}]$, as

$$S(x) = \frac{p_i^*(z)}{q_i^*(z)}, \quad x \in [x_i, x_{i+1}], \tag{3.4}$$

where $z = (x - x_i)/h_i$, $h_i = x_{i+1} - x_i$,

$$\begin{aligned} p_i^*(z) &= u_i f_i(1-z)^3 + [(u_i + w_i)f_i + h_i u_i d_i]z(1-z)^2 \\ &\quad + [(v_i + w_i)f_{i+1} - h_i v_i d_{i+1}]z^2(1-z) + v_i f_{i+1} z^3, \end{aligned}$$

$$q_i^*(z) = u_i(1-z)^2 + w_i z(1-z) + v_i z^2.$$

Remark 3.2. When $u_i = v_i = 1$ and $w_i = 2$, the RCFIF reduces to the standard cubic Hermite FIF:

$$\begin{aligned}\Phi(L_i(x)) = {} & \alpha_i\Phi(x) + (f_i - \alpha_i f_1)(1-\theta)^3 \\ & + \{3(f_i - \alpha_i f_1) + \ell(a_i d_i - \alpha_i d_1)\}\theta(1-\theta)^2 \\ & + \{3(f_{i+1} - \alpha_i f_n) - \ell(a_i d_{i+1} - \alpha_i d_n)\}\theta^2(1-\theta) + (f_{i+1} - \alpha_i f_n)\theta^3,\end{aligned}$$

studied in depth in **[15]**.

Remark 3.3. The RCFIF (3.2) can be rewritten in the form:

$$\Phi(L_i(x)) = \alpha_i\Phi(x) + f_i(1-\theta) + f_{i+1}\theta + \frac{\ell[u_i(d_i - \triangle_i) + v_i(\triangle_i - d_{i+1})]}{q_i(\theta)},$$

where $\triangle_i = (f_{i+1} - f_i)/\ell$. If $u_i \to \infty$ and $v_i \to \infty$, then our RCFIF reduces to the affine cubic FIF:

$$\Phi(L_i(x)) = \alpha_i\Phi(x) + (f_i - \alpha_i f_1)(1-\theta) + (f_{i+1} - \alpha_i f_n)\theta.$$

If $\alpha_i \to 0^+$, then the affine RCFIF transforms into a straight line segment in the interval $[x_i, x_{i+1}]$. Hence, the RCFIF may be used to preserve the fundamental shape properties of interpolation data.

4. Convergence analysis. In this section, we deduce the error bound for the uniform distance between the developed RCFIF and the data generating function Ψ in $\mathcal{C}^k$, $k = 1, 3$. Due to the implicit expression of the RCFIF Φ, it is difficult to compute the uniform error bound $\|\Phi - \Psi\|_\infty$ by using any standard numerical analysis techniques. Hence, we derive an upper bound of the uniform error through the use of the classical counterpart S (of Φ) with the aid of

$$\|\Phi - \Psi\|_\infty \le \|\Phi - S\|_\infty + \|S - \Psi\|_\infty, \tag{4.1}$$

where S is given by (3.4).

Theorem 4.1. *Let Ψ be the original function, and let S be the classical rational cubic interpolant defined in* (3.4). *For $x \in [x_i, x_{i+1}]$, the following hold.*

(a) *If* $\Psi \in \mathcal{C}^1[x_1, x_n]$, *then*

(4.2)
$$|S(x) - \Psi(x)| \le \frac{h}{K^*}(u^* + v^*)\|\Psi^{(1)}\|_\infty + \frac{h}{4K^*} \max_{1\le i\le n-1}\{u^*|d_i|, v^*|d_{i+1}|\},$$

where $K^* = \min_{1\le i\le n-1} |q_i^*(z)|$, $u^* = \max_{1\le i\le n-1} u_i$, $v^* = \max_{1\le i\le n-1} v_i$, *and* $h = \max_{1\le i\le n-1} h_i$.

(b) *If* $\Psi \in \mathcal{C}^3[x_1, x_n]$, *then*

$$|\Psi(x) - S(x)| \le \|\Psi^{(3)}\|_{\infty,i} h_i^3 c_i, \quad x \in [x_i, x_{i+1}], \tag{4.3}$$

where $\|\cdot\|_{\infty,i}$ *denotes the uniform norm on* $[x_i, x_{i+1}]$,

$$c_i = \max_{0\le z\le 1} \Theta(v_i, w_i, z),$$

$$\Theta(v_i, w_i, z) = \begin{cases} \max \Theta_1(v_i, w_i, z) & \text{for } 0 \le z \le z^*,\ v_i < w_i, \\ \max \Theta_2(v_i, w_i, z) & \text{for } z^* \le z \le 1,\ v_i < w_i, \\ \max \Theta_3(v_i, w_i, z) & \text{for } 0 \le z \le 1,\ v_i > w_i, \end{cases}$$

$z^* = 1 - v_i/w_i$, *and* $\Theta_1(v_i, w_i, z)$, $\Theta_2(v_i, w_i, z)$ *and* $\Theta_3(v_i, w_i, z)$ *are defined in* (4.9), (4.11) *and* (4.13), *respectively.*

Proof. From (3.4), we observe that

$$S(x) - \Psi(x) = [p_i^*(z) - q_i^*(z)\Psi(x)]/q_i^*(z), \quad x \in [x_i, x_{i+1}].$$

Consequently,

$$\begin{aligned} |S(x) - \Psi(x)| &\le \frac{1}{|q_i^*(z)|}[|(1-z)^3 u_i + z(1-z)^2(u_i + w_i)||f_i - \Psi(x)| \\ &\qquad + |z^2(1-z)(v_i + w_i) + z^3 v_i||f_{i+1} - \Psi(x)| \\ &\qquad + \ell|z(1-z)^2 u_i d_i - z^2(1-z)v_i d_{i+1}|] \\ &\le \frac{1}{K^*}\Big[\max|u_i| \max|f_i - \Psi(x)| + \max|v_i| \max|f_{i+1} - \Psi(x)| \\ &\qquad + \frac{h_i}{4}\max\{\max|u_i d_i|, \max|v_i d_{i+1}|\Big] \\ &\le \frac{1}{K^*}(u^* + v^*)\Omega(\Psi, h) + \frac{h}{4K^*}\max\{u^*|d_i|, v^*|d_{i+1}|\}, \end{aligned}$$

where $\Omega(\Psi, h)$ is the modulus of continuity of Ψ. Since $\Psi \in \mathcal{C}^1[x_1, x_n]$, it is clear that, see for instance, **[27]**,

$$\Omega(\Psi, h) \leq h\|\Phi^{(1)}\|_\infty. \tag{4.4}$$

This completes the proof of (a).

Now, the error estimation in (b) between the original function $\Psi \in \mathcal{C}^3[x_1, x_n]$ and the classical rational cubic function S in an arbitrary subinterval $I_i = [x_i, x_{i+1}]$ can be found by using the Peano-Kernel theorem. The pointwise error in each subinterval I_i is given by

$$R[\Psi] = \Psi(x) - P(x) = \frac{1}{2}\int_{x_i}^{x_{i+1}} \Psi^{(3)}(\tau) R_x[(x-\tau)_+^2]\, d\tau. \tag{4.5}$$

Since $\Psi \in \mathcal{C}^3(I)$, (4.5) yields

$$|\Psi(x) - P(x)| \leq \frac{1}{2}\|\Psi^{(3)}\|_{\infty,i}\int_{x_i}^{x_{i+1}} |R_x[(x-\tau)_+^2]|\, d\tau. \tag{4.6}$$

Here, $R_x[(x-\tau)_+^2]$ is called the Peano-Kernel, which is given by

$$R_x[(x-\tau)_+^2] = \begin{cases} r(\tau, x) & \text{for } x_i < \tau < t, \\ s(\tau, x) & \text{for } t < \tau < x_{i+1}, \end{cases}$$

where

$$\begin{aligned} r(\tau, x) &= (x-\tau)^2 \\ &\quad - \frac{z^2}{q_i^*(z)}[(v_i + w_i(1-z))(x_{i+1}-\tau)^2 - 2h_i(1-z)v_i(x_{i+1}-\tau)], \\ s(\tau, x) &= -\frac{z^2}{q_i^*(z)}[(v_i + w_i(1-z))(x_{i+1}-\tau)^2 - 2h_i(1-z)v_i(x_{i+1}-\tau)]. \end{aligned}$$

It is clear that $r(\tau, x) - s(\tau, x) = (x-\tau)^2$, $x \in [x_1, x_n]$.

The integral $\int_{x_i}^{x_{i+1}} |R_x[(x-\tau)_+^2]|\, d\tau$ can be expressed as

$$\int_{x_i}^{x_{i+1}} |R_x[(x-\tau)_+^2]|\, d\tau = \int_{x_i}^{t} |r(x, \tau)|\, d\tau + \int_{t}^{x_{i+1}} |s(x, \tau)|\, d\tau. \tag{4.7}$$

The roots of $r(x, x) = 0$ and $s(x, x) = 0$ are $0, 1 - (v_i/w_i)$ and 1. These roots lie in $[0, 1]$ for all $v_i > 0$ and $w_i > 0$. The roots of $r(x, \tau) = 0$ are

$\tau_j = x - h_i(B + (-1)^{j+1}D)/A$, $j = 1, 2$, where

$$A = q_i^*(z) - z^2(1-z)[v_i + w_i(1-z)],$$
$$B = [v_i + w_i(1-z)](1-z) - v_i,$$
$$C = [v_i + w_i(1-z)](1-z) - 2v_i$$

and

$$D = \sqrt{B^2 - AC}.$$

The roots of $s(x,\tau) = 0$ are $\tau_3 = x_{i+1} - (2h_i v_i(1-z))/(v_i + w_i(1-z))$ and $\tau_4 = x_{i+1}$.

Case 1. $0 \le z \le z^*$ and $v_i < w_i$. Here, (4.7) takes the form

$$|\Psi(x) - S(x)| \le \frac{1}{2}\|\Psi^{(3)}\|_{\infty,i} h_i^3 \Theta_1(v_i, w_i, z), \tag{4.8}$$

where

$$\begin{aligned}\Theta_1(v_i, w_i, z) &= \int_{x_i}^{t} |r(x,\tau)|\, d\tau + \int_{t}^{x_{i+1}} |s(x,\tau)|\, d\tau,\\ &= -\int_{x_i}^{\tau_1} r(x,\tau)\, d\tau + \int_{\tau_1}^{t} r(x,\tau)\, d\tau\\ &\quad - \int_{t}^{\tau_3} s(x,\tau)\, d\tau + \int_{\tau_3}^{\tau_4} s(x,\tau)\, d\tau.\end{aligned}$$

Integrating and simplifying the above expression, we obtain

$$\begin{aligned}&\Theta_1(v_i, w_i, z)\\ &= \frac{h_i^3}{q_i(z)}\Bigg\{\frac{Az^3}{3} - Bz^2 + Cz - \frac{2(B+D)^2}{3A^2} + \frac{2B(B+D)^2}{A^2}\\ &\qquad - \frac{2C(B+D)}{A}\\ &\qquad + z^2(1-z)^2\left[\frac{2v_i - w_i(1-z)}{3} - \frac{8v_i^3}{3[v_i + w_i(1-z)]^2}\right]\Bigg\}.\end{aligned} \tag{4.9}$$

Case 2. $z \le z^* \le 1$ and $v_i < w_i$. Here, (4.7) takes the form

$$|\Psi(x) - S(x)| \le \frac{1}{2}\|\Psi^{(3)}\|_{\infty,i} h_i^3 \Theta_2(v_i, w_i, z), \tag{4.10}$$

where

$$\begin{aligned}\Theta_2(v_i,w_i,z) &= \int_{x_i}^{t} |r(x,\tau)|\,d\tau + \int_{t}^{x_{i+1}} |s(x,\tau)|\,d\tau,\\ &= \int_{x_i}^{\tau_1} r(x,\tau)\,d\tau - \int_{\tau_1}^{\tau_2} r(x,\tau)\,d\tau\\ &\quad - \int_{\tau_2}^{x} r(x,\tau)\,d\tau + \int_{x}^{\tau_4} s(x,\tau)\,d\tau.\end{aligned}$$

Integrating and simplifying the above expression, we obtain

(4.11)

$$\begin{aligned}\Theta_2(v_i,w_i,z) = \frac{h_i^3}{q_i(z)}\Bigg\{ &\frac{Az^3}{3} - Bz^2 + Cz - \frac{2(B+D)^2}{3A2} + \frac{2B(B+D)^2}{A^2}\\ &- \frac{2C(B+D)}{A} + \frac{2(B-D)^2}{3A^2} - \frac{2B(B-D)^2}{A^2}\\ &+ \frac{2C(B-D)}{A} + z^2(1-z)^3\left[\frac{4v_i + w_i(1-z)}{3}\right]\Bigg\}.\end{aligned}$$

Case 3. $0 \le z \le 1$ and $v_i > w_i$. Here, (4.7) takes the form

$$|\Psi(x) - S(x)| \le \frac{1}{2}\|\Psi^{(3)}\|_{\infty,i} h_i^3 \Theta_3(v_i,w_i,z), \tag{4.12}$$

where

$$\begin{aligned}\Theta_3(v_i,w_i,z) &= \int_{x_i}^{t} |r(x,\tau)|\,d\tau + \int_{t}^{x_{i+1}} |s(x,\tau)|\,d\tau,\\ &= \int_{x_i}^{x} r(x,\tau)\,d\tau + \int_{x}^{\tau_4} s(x,\tau)\,d\tau.\end{aligned}$$

Integrating and simplifying the above expression, we obtain

(4.13)

$$\Theta_3(v_i,w_i,z) = \frac{h_i^3}{q_i(z)}\left\{\frac{Az^3}{3} - Bz^2 + Cz + z^2(1-z)^3\left[\frac{4v_i + w_i(1-z)}{3}\right]\right\}.$$

Thus, the upper bound of the pointwise error between the original interpolant and the classical rational cubic interpolant follows from (4.8)–(4.13). □

Theorem 4.2. *Let* Φ *be the* $\mathcal{C}^1$-RCFIF *and* Ψ *the data generating function for the given data* $\{(x_j, f_j),\ j \in \Lambda^*\}$. *Let* d_j *be the bounded*

first order derivative at the knot x_j, $j \in \Lambda^*$. *Suppose the shape parameters satisfy* $u_i > 0$, $v_i > 0$ *and* $w_i > \max\{u_i, v_i\}$ *for* $i \in \Lambda$. *Let*

$$u^* = \max_{1\le i\le n-1} u_i, \qquad v^* = \max_{1\le i\le n-1} v_i, \qquad K^* = \min_{1\le i\le n-1} |q_i(z)|,$$
$$h = \max_{1\le i\le n-1} h_i, \qquad E(h) = \|\Psi\|_\infty + 2hE_1, \qquad E^*(h) = F + 2hE_2,$$
$$E_1 = \max_{1\le j\le n} |d_j|, \qquad F = \max\{|f_1|, |f_n|\}, \qquad E_2 = \max\{|d_1|, |d_n|\}.$$

Then, the following estimates are valid:

(a) *If* $\Psi \in \mathcal{C}^1[x_1, x_n]$, *then*

(4.14)
$$\|\Psi - \Phi\|_\infty \le \frac{h}{K^*}(u^* + v^*)\|\Psi^{(1)}\|_\infty + \frac{h}{4K^*}\max\{u^*|d_i|, v^*|d_{i+1}|\} + \frac{|\alpha|_\infty}{1 - |\alpha|_\infty}(E(h) + E^*(h)).$$

(b) *If* $\Psi \in \mathcal{C}^3[x_1, x_n]$, *then*

$$\|\Psi - \Phi\|_\infty \le \|\Psi^{(3)}\|_\infty h^3 c + \frac{|\alpha|_\infty}{1 - |\alpha|_\infty}(E(h) + E^*(h)), \tag{4.15}$$

where

$$c = \max_{1\le i\le n-1} c_i;$$

and c_i *is defined in Theorem* 4.1.

Proof. Consider the space

$$\mathcal{F}^* = \{g \in C^1(I, \mathbb{R}) \mid g(x_1) = f_1,\ g(x_n) = f_n, g'(x_1) = d_1, g'(x_n) = d_n\}.$$

From (2.2) and (3.2), the Read-Bajraktarević operator

$$T^*_\alpha : \mathcal{F}^* \longrightarrow \mathcal{F}^*$$

for the RCFIF can be written as

$$T^*_\alpha g(x) = \alpha_i g(L_i^{-1}(x)) + \frac{p_i(L_i^{-1}(x), \alpha_i)}{q_i(L_i^{-1}(x))}, \quad x \in I_i,\ i \in \Lambda. \tag{4.16}$$

Note that Φ is the fixed point of T^*_α with $\alpha \neq \mathbf{0}$ and S is the fixed point of $T^*_{\mathbf{0}}$. Since T^*_α is a contractive operator with the contraction factor

$|\alpha|_\infty$, we have

$$\|T_\alpha^*\Phi - T_\alpha^* S\|_\infty \le |\alpha|_\infty \|\Phi - S\|_\infty. \tag{4.17}$$

From (4.16), we have

$$|T_\alpha^* S(x) - T_{\mathbf{0}}^* S(x)| \le |\alpha|_\infty \left(\|S\|_\infty + \left| \frac{\partial\{(p_i(L_i^{-1}(x), \tau_i))/(q_i(L_i^{-1}(x)))\}}{\partial \alpha_i} \right| \right), \tag{4.18}$$

$$|\tau_i| \in (0, \alpha_i),$$

where the mean value theorem for the functions of several variables is used in this calculation.

Now, we wish to discover the error bounds of the terms on the right side of (4.18). From the classical rational cubic function (3.4), it is easy to see that

$$\begin{aligned} S(x) = {} & \sigma_1(u_i, v_i, w_i, z) f_i + \sigma_2(u_i, v_i, w_i, z) f_{i+1} \\ & + \sigma_3(u_i, v_i, w_i, z)\, d_i - \sigma_4(u_i, v_i, w_i, z)\, d_{i+1}, \end{aligned} \tag{4.19}$$

where

$$\begin{aligned} \sigma_1(u_i, v_i, w_i, z) &= \frac{1}{q_i(z)} \{u_i(1-z)^3 + w_i z(1-z)^2\} \ge 0, \\ \sigma_2(u_i, v_i, w_i, z) &= \frac{1}{q_i(z)} \{w_i z^2(1-z) + v_i z^3\} \ge 0, \\ \sigma_3(u_i, v_i, w_i, z) &= \frac{h_i}{q_i(z)} \{u_i z(1-z)^2\} \ge 0, \\ \sigma_4(u_i, v_i, w_i, z) &= \frac{h_i}{q_i(z)} \{v_i z^2(1-z)\} \ge 0. \end{aligned}$$

It is also easy to verify that $\sigma_1(u_i, v_i, w_i, z) + \sigma_2(u_i, v_i, w_i, z) = 1$. In addition, for $u_i > 0$, $v_i > 0$, $w_i > 0$, and the choice of $w_i > \max\{u_i, v_i\}$, we obtain the following inequality:

$$\begin{aligned} \sigma_3(u_i, v_i, w_i, z) + \sigma_4(u_i, v_i, w_i, z) &= \frac{h_i}{q_i(z)} \{u_i z(1-z)^2 + v_i z^2(1-z)\} \\ &\le h_i \left\{ \frac{u_i z(1-z)^2}{w_i z(1-z)^2} + \frac{v_i z^2(1-z)}{w_i z^2(1-z)} \right\} \\ &= h_i \left\{ \frac{u_i}{w_i} + \frac{v_i}{w_i} \right\} \le 2h_i. \end{aligned}$$

Using the above results in (4.19), we obtain

$$|S(x)| \le \max_{j=i,i+1}\{|f_j|\} + 2h_i \max_{j=i,i+1}\{|d_j|\}.$$

Since the above inequality is true for all $i \in \Lambda$, we obtain the following estimation:

$$\|S\|_\infty \le E(h) := \|\Psi\|_\infty + 2hE_1. \tag{4.20}$$

Since $q_i(x)$ is independent of α_i, from the first term on the right side of (4.18),

$$\frac{\partial\{(p_i(L_i^{-1}(x),\tau_i))/(q_i(L_i^{-1}(x)))\}}{\partial\alpha_i} = \sigma_1(u_i,v_i,w_i,z)f_1 + \sigma_2(u_i,v_i,w_i,z)f_n + \sigma_3(u_i,v_i,w_i,z)d_1 - \sigma_4(u_i,v_i,w_i,z)\,d_n.$$

Now, by applying a similar argument, the following bound can be obtained:

$$\left|\frac{\partial\{(p_i(L_i^{-1}(x),\tau_i))/(q_i(L_i^{-1}(x)))\}}{\partial\alpha_i}\right| \le E^*(h) := F + 2hE_2. \tag{4.21}$$

Substituting (4.20) and (4.21) in (4.18), we have

$$|T_\alpha^* S(x) - T_{\mathbf{0}}^* S(x)| \le |\alpha|_\infty (E(h) + E^*(h)), \quad x \in [x_i, x_{i+1}].$$

Since the above result is valid in every subinterval, we get

$$\|T_\alpha^* S - T_{\mathbf{0}}^* S\|_\infty \le |\alpha|_\infty (E(h) + E^*(h)). \tag{4.22}$$

Using (4.17) and (4.22) in

$$\|\Phi - S\|_\infty = \|T_\alpha^*\Phi - T_{\mathbf{0}}^* S\|_\infty \le \|T_\alpha^*\Phi - T_\alpha^* S\|_\infty + \|T_\alpha^* S - T_{\mathbf{0}}^* S\|_\infty,$$

we have the following estimate:

$$\|\Phi - S\|_\infty \le \frac{|\alpha|_\infty (E(h) + E^*(h))}{1 - |\alpha|_\infty}. \tag{4.23}$$

Using the results of Theorem 4.1 and (4.23) in (4.1), we obtain the desired upper bounds in (4.14)–(4.15). □

4.1. Convergence result. Assume that $\max_{1\le j\le n}|d_j|$ is bounded and $K^* > \delta$, for every partition of the domain I, where δ is a real positive number. Since $\alpha_i < a_i$ implies that $|\alpha|_\infty < h/\ell$, Theorem 4.2 proves that the RCFIF Φ uniformly converges to the original function

Ψ as $h \to 0$. Additionally, if $|\alpha_i| < a_i^3 = h_i^3/\ell^3$ for $i \in \Lambda$, then $\|\Psi - \Phi\|_\infty = O(h^3)$ as $h \to 0$.

5. Constrained $\mathcal{C}^1$-RCFIF. In this section, we discuss the construction of constrained RCFIFs whose graphs lie strictly in between two piecewise straight lines L^u and L^b when the given interpolation data is found to be distributed between L^u and L^b. In general, an RCFIF may not lie in between L^u and L^b with an arbitrary choice of IFS parameters. In order to avoid this circumstance, we deduce sufficient data-dependent restrictions on the scaling factor α_i and on the shape parameters u_i, v_i and w_i in subsection 5.1 so that the RCFIF preserves the shape of the constrained data. Examples of constrained $\mathcal{C}^1$-RCFIFs are discussed in subsection 5.2.

5.1. Theory of the constrained RCFIF. Suppose that the line L^u is defined piecewise over $[x_i, x_{i+1}]$ such that $L^u(x_j) = f_j^u$ for all $j \in \Lambda^*$. Similarly, L^b is defined piecewise over $[x_i, x_{i+1}]$ such that $L^b(x_j) = f_j^b$ for all $j \in \Lambda^*$. The IFSs for L^u and L^b over I are given, respectively, by $\{\mathbb{R}; (L_i(x), F_i^u(x)),\ i \in \Lambda\}$ and $\{\mathbb{R}; (L_i(x), F_i^b(x)),\ i \in \Lambda\}$, where

$$F_i^u(x) = (1-\theta)\mu_i + \theta\eta_i,$$
$$F_i^b(x) = (1-\theta)\mu_i^* + \theta\eta_i^*,$$

$$\theta = \frac{x - x_1}{x_n - x_1},$$

$$\mu_i = m_i x_i + c_i, \eta_i = m_i x_{i+1} + c_i,$$

$$\mu_i^* = m_i^* x_i + c_i^*,$$

and

$$\eta_i^* = m_i^* x_{i+1} + c_i^*, \quad i \in \Lambda.$$

Let $\{(x_j, f_j) : j \in \Lambda^*\}$ be the given set of data points lying strictly in between the straight lines L^u and L^b. Then,

$$m_j^* x_j + c_j^* = L^b(x_j) < f_j < L^u(x_j) = m_j x_j + c_j \quad \text{for all } j \in \Lambda$$

and

$$m_{n-1}^* x_n + c_{n-1}^* < f_n < m_{n-1} x_n + c_{n-1}.$$

Since L^u and L^b are the FIFs associated with the IFSs $\{\mathbb{R}; (L_i(x), F_i^u(x)), i \in \Lambda\}$ and $\{\mathbb{R}; (L_i(x), F_i^b(x)),\ i \in \Lambda\}$, respectively, then the functional equations of L^u and L^b are

$$\begin{aligned} L^u(L_i(x)) &= m_i L_i(x) + c_i = \mu_i(1-\theta) + \eta_i\theta = r_i(\theta) \quad \text{(say)},\\ L^b(L_i(x)) &= m_i^* L_i(x) + c_i^* = \mu_i^*(1-\theta) + \eta_i^*\theta = r_i^*(\theta) \quad \text{(say)}, \end{aligned} \tag{5.1}$$

where $L_i(x) = a_i x + b_i$ with $a_i = (x_{i+1} - x_i)/(x_n - x_1)$ and $b_i = (x_n x_i - x_1 x_{i+1})/(x_n - x_1)$, $\theta = (x - x_1)/\ell$, $\ell = x_n - x_1$.

Note that, at $x = x_1$, $\mu_i = m_i x_i + c_i$, $\mu_i^* = m_i^* x_i + c_i^*$ and at $x = x_n$, $\eta_i = m_i x_{i+1} + c_i$, $\eta_i^* = m_i^* x_{i+1} + c_i^*$. Thus, the $\mathcal{C}^1$-RCFIF Φ will lie strictly in between the piecewise straight lines L^u and L^b if

$$L^b(L_i(x)) < \Phi(L_i(x)) < L^u(L_i(x)) \quad \text{for all } x \in [x_1, x_n],\ i \in \Lambda. \tag{5.2}$$

Let $\theta_j = (x_j - x_1)/(x_n - x_1)$, $r_i^j = r_i(\theta_j)$ and $r_i^{*j} = r_i^*(\theta_j)$. Assume that $\alpha_i \in [0, a_i)$, $i \in \Lambda$ as $\Phi \in \mathcal{C}^1[x_1, x_n]$. The RCFIF Φ will lie between the piecewise straight lines L^u and L^b, it is clear from (5.2) that, for the next generation of interpolation points, the following inequalities should be satisfied:

$$r_i(\theta_j) < \Phi(L_i(x_j)) < r_i^*(\theta_j) \Longrightarrow r_i^j < \Phi(L_i(x_j)) < r_i^{*j}. \tag{5.3}$$

However, from (5.2), we have

$$\alpha_i r_i^j + \frac{p_i(\theta_j)}{q_i(\theta_j)} < \alpha_i f_j + \frac{p_i(\theta_j)}{q_i(\theta_j)} < \alpha_i r_i^{*j} + \frac{p_i(\theta_j)}{q_i(\theta_j)}.$$

For the validity of $r_i^j < \alpha_i f_j + (p_i(\theta_j)/q_i(\theta_j)) < r_i^{*j}$, we need to impose the following conditions from (5.3):

$$r_i^j < \alpha_i r_i^j + \frac{p_i(\theta_j)}{q_i(\theta_j)} \quad \text{and} \quad \alpha_i r_i^{*j} + \frac{p_i(\theta_j)}{q_i(\theta_j)} < r_i^{*j}.$$

Therefore, the RCFIF lies in between the straight lines L^u and L^b if

$$\Omega_{1,i}(\theta_j) := (\alpha_i - 1) r_i^j + \frac{p_i(\theta_j)}{q_i(\theta_j)} \geq 0 \tag{5.4}$$

for all $\theta \in [0, 1]$, $i \in \Lambda$, $j \in \Lambda^*$, and

$$\Omega_{2,i}(\theta_j) := (\alpha_i - 1) r_i^{*j} + \frac{p_i(\theta_j)}{q_i(\theta_j)} \leq 0 \tag{5.5}$$

for all $\theta \in [0,1]$, for every $i \in \Lambda$, $j \in \Lambda^*$. After some algebraic simplifications, $\Omega_{1,i}(\theta)$ is reformulated as

$$\Omega_{1,i}(\theta_j) = \frac{p_i^*(\theta_j)}{q_i(\theta_j)} > 0, \tag{5.6}$$

$$p_i^*(\theta_j) = (1-\theta_j)^3 U_i^* + \theta_j(1-\theta_j)^2 V_i^* + \theta_j^2(1-\theta_j) W_i^* + \theta_j^3 X_i^*,$$
$$U_i^* = U_i + u_i(\alpha_i - 1)r_i^j,\ V_i^* = V_i + (u_i + w_i)(\alpha_i - 1)r_i^j,$$
$$W_i^* = W_i + (v_i + w_i)(\alpha_i - 1)r_i^j,\ X_i^* = X_i + v_i(\alpha_i - 1)r_i^j.$$

Clearly, the shape parameters $u_i > 0$, $v_i > 0$ and $w_i > 0$ guarantee that the denominator in (5.6) is positive. Thus, the RCFIF preserves the constrained aspect of the constrained data if the numerator $p_i^*(\theta_j)$ is positive, which is sufficient to show that the expressions U_i^*, V_i^*, W_i^* and X_i^* are positive.

Since $u_i > 0$ and

$$U_i^* = U_i + u_i(\alpha_i - 1)r_i^j = u_i(f_i - \alpha_i f_1 + (\alpha_i - 1)r_i^j), \quad j \in \Lambda^*,$$

the choice of

$$\alpha_i < \Xi_i := \min\left\{ \frac{f_i - r_i^j}{f_1 - r_i^j} :\ j \in \Lambda^* \right\} \quad \text{yields } U_i^* > 0.$$

Similarly, since $v_i > 0$ and

$$X_i^* = X_i + v_i(\alpha_i - 1)r_i^j = v_i(f_{i+1} - \alpha_i f_n + (\alpha_i - 1)r_i^j), \quad j \in \Lambda^*,$$

the selection of

$$\alpha_i < \eth_i := \min\left\{ \frac{f_{i+1} - r_i^j}{f_n - r_i^j} :\ j \in \Lambda^* \right\}$$

ensures $X_i^* > 0$. Consider $V_i^* = V_i + w_i(\alpha_i - 1)r_i^j = w_i(f_i - \alpha_i f_1 + (\alpha_i - 1)r_i^j) + \ell u_i(a_i d_i - \alpha_i d_1)$. Then, for $a_i d_i - \alpha_i d_1 > 0$, arbitrary $u_i > 0$ and $w_i > 0$, provide $V_i^* > 0$. Otherwise, for $u_i > 0$, the choice of

$$w_i > \Upsilon_i := \max\left\{ \frac{-\ell u_i(a_i d_i - \alpha_i d_1)}{f_i - \alpha_i f_1 + (\alpha_i - 1)r_i^j} :\ j \in \Lambda^* \right\}$$

results in $V_i^* > 0$. Similarly, consider

$$W_i^* = W_i + w_i(\alpha_i - 1)r_i^j = w_i(f_{i+1} - \alpha_i f_n + (\alpha_i - 1)r_i^j) - \ell v_i(a_i d_{i+1} - \alpha_i d_n).$$

Then, for $(a_i d_{i+1} - \alpha_i d_n) < 0$, arbitrary $v_i > 0$ and $w_i > 0$, provide $X_i^* > 0$. Otherwise, for $v_i > 0$, the selection of

$$w_i > \aleph_i := \max\left\{ \frac{\ell v_i (a_i d_{i+1} - \alpha_i d_n)}{f_{i+1} - \alpha_i f_n + (\alpha_i - 1) r_i^j} : \ j \in \Lambda^* \right\}$$

ensures $W_i^* > 0$. Hence, $\Omega_{1,i}(\theta_j) > 0$ for all $i \in \Lambda$, $j \in \Lambda^*$, when

- the scaling factors are chosen as

$$\alpha_i < \alpha_i^u := \min\{a_i, \ \Xi_i, \ \Im_i\}; \tag{5.7}$$

- the shape parameters are chosen as $u_i > 0$, $v_i > 0$; and

$$w_i > w_i^u := \max\{0, \ \Upsilon_i, \ \aleph_i\}. \tag{5.8}$$

Using similar arguments as above, we deduce that $\Omega_{2,i}(\theta_j) < 0$ for all $\theta \in [0,1]$, $i \in \Lambda$, $j \in \Lambda^*$, i.e., the RCFIF Φ lies below the straight line L^u when

- the scaling factors are selected as

$$\alpha_i < \alpha_i^b := \min\{a_i, \ \Xi_i^*, \ \Im_i^*\}; \tag{5.9}$$

- the shape parameters are selected as $u_i > 0$, $v_i > 0$; and

$$w_i > w_i^b := \max\{0, \ \Upsilon_i^*, \ \aleph_i^*\}, \tag{5.10}$$

where

$$\Xi_i^* := \min\left\{ \frac{r_i^{*j} - f_i}{r_i^{*j} - f_1} : \ j \in \Lambda^* \right\},$$

$$\Im_i^* := \min\left\{ \frac{r_i^{*j} - f_{i+1}}{r_i^{*j} - f_n} : \ j \in \Lambda^* \right\},$$

$$\Upsilon_i^* = \max\left\{ \frac{-\ell u_i (a_i d_i - \alpha_i d_1)}{f_i - \alpha_i f_1 + (\alpha_i - 1) r_i^{*j}} : \ j \in \Lambda^* \right\}$$

and

$$\aleph_i^* = \max\left\{ \frac{\ell v_i (a_i d_{i+1} - \alpha_i d_n)}{f_{i+1} - \alpha_i f_n + (\alpha_i - 1) r_i^{*j}} : \ j \in \Lambda^* \right\}.$$

Thus, the RCFIF preserves the constraining nature of given data and lies between the straight lines if the IFS parameters are selected

according to (5.11) and (5.12). The above discussion is encapsulated in the next theorem.

Theorem 5.1. *Let* Φ *be the* RCFIF (3.2) *defined over the interval* $[x_1, x_n]$ *with respect to the given data* $\{(x_j, y_j),\ j \in \Lambda^*\}$. *Further assume that the data points lie above the piecewise straight line* L^b *and below the piecewise straight line* L^u. *Then, the* RCFIF Φ *lies in between those piecewise straight lines* L^u *and* L^b *if the following conditions are satisfied for all* $i \in \Lambda$:

(i) *select the scaling factors as*

$$0 < \alpha_i < \min\{\alpha_i^u, \alpha_i^b\}; \tag{5.11}$$

(ii) *select the shape parameters as*

$$u_i > 0, \qquad v_i > 0 \quad \textit{and} \quad w_i > \max\{w_i^u, w_i^b\}, \tag{5.12}$$

where α_i^u, w_i^u, α_i^b *and* w_i^b *are defined in* (5.7)–(5.10), *respectively.*

Remark 5.2. It is clear that the positivity preserving interpolation is a special case of the above constrained interpolation scheme. By considering $r_i^j = 0$ in (5.4) and $r_i^{*j} = \infty$ in (5.5) for $i \in \Lambda$, $j \in \Lambda^*$, then the data lies above the x-axis, i.e., the data is positive such that the RCFIF (3.2) preserves the positivity feature of the given data with respect to the restricted IFS parameters calculated from Theorem 5.1. Since $r_i^{*j} = \infty$, there is no need of captivating the RCFIF from above by a piecewise straight line.

5.2. Numerical example. A numerical example is presented here to illustrate the construction of the $\mathcal{C}^1$-RCFIFs and the related constrained interpolation problem discussed in the previous subsection. For this, we consider the interpolating data set $\{(0,1), (1,0.7), (2,0.8), (3,0.6), (4,0.9)\}$ which is constrained in between the two piecewise straight lines taken as:

$$L^u = \begin{cases} -0.3x + 1.1 & 0 \le x \le 1, \\ 0.1x + 0.7 & 1 \le x \le 2, \\ -0.2x + 1.3 & 2 \le x \le 3, \\ 0.3x - 0.2 & 3 \le x \le 4, \end{cases} \tag{5.13}$$

$$L^b = \begin{cases} -0.3x + 0.9 & 0 \le x \le 1, \\ 0.1x + 0.5 & 1 \le x \le 2, \\ -0.2x + 1.1 & 2 \le x \le 3, \\ 0.3x - 0.4 & 3 \le x \le 4. \end{cases}$$

TABLE 1. Scaling factors and shape parameters used in the RCFIFs.

Fig.	Scaling factors (α)	Shape parameters (w)
1(a)	$\alpha = (0.6, 0.24, 0.24, -0.24)$	$w = (18.0000, 2.7937, 2.0580, 1.9489)$
1(b)	$\alpha = (0.24, 0.24, 0.24, 0.24)$	$w = (2.2841, 2.7937, 2.0580, 1.6134)$
1(c)	$\alpha = (\mathbf{0.01}, 0.24, 0.24, 0.24)$	$w = (\mathbf{1.1926}, 2.7937, 2.0580, 1.6134)$
1(d)	$\alpha = (0.24, \mathbf{0.01}, 0.24, 0.24)$	$w = (2.2841, \mathbf{0.7416}, 2.0580, 1.6134)$
1(e)	$\alpha = (0.24, \mathbf{0.01}, 0.24, 0.24)$	$w = (2.2841, \mathbf{100.7937}, 0.5952, 1.6134)$
1(f)	$\alpha = (\mathbf{0.01}, \mathbf{0.01}, \mathbf{0.01}, \mathbf{0.01})$	$w = (\mathbf{100}, \mathbf{102}, \mathbf{100}, \mathbf{100})$
1(g)	$\alpha = (\mathbf{0.01}, \mathbf{0.01}, \mathbf{0.01}, \mathbf{0.01})$	$w = (\mathbf{1.1926}, \mathbf{0.7416}, \mathbf{0.5952}, \mathbf{1.3889})$
1(h)	$\alpha = (0, 0, 0, 0)$	$w = (1.2143, 0.7500, 0.6667, 1.4167)$

The derivative values at the knots are calculated using the arithmetic mean method. We have iteratively generated eight $\mathcal{C}^1$-RCFIFs using the IFS parameters given in Table 1. For simplicity, we fixed two of the shape parameters $u_i = 1$ and $v_i = 1$, $i = 1, 2, 3, 4$. For an arbitrary choice of rational IFS parameters, the RCFIF Φ_1 may not preserve the constrained nature of the given data, see for instance, Figure 1(a). Thus, by implementing Theorem 5.1, we have calculated the restrictions on the IFS parameters that satisfy the constrained inequalities (5.11) and (5.12) such that the RCFIF (3.2) must be $\mathcal{C}^1$-continuous in $[0, 4]$ and bounded between the upper straight line L^u and the lower straight line L^b. The choice of scaling factors and shape parameters as per Theorem 5.1 are shown in Table 1. Figure 1(b) is generated as the graph of such an RCFIF Φ_2 which preserves the constrained nature of given data for specific restricted IFS parameters. Figure 1(b) is used as the standard reference curve.

Figures 1(c)–1(g) are generated by modifying the rational IFS parameters as shown in boldface letters in Table 1. The constrained RCFIF Φ_3 in Figure 1(c) is generated with a perturbation in the scaling factor α_1, and it has major effects in first subinterval, while the changes in second subinterval are also noticeable in comparison with Φ_2. These effects are distributed according to the code space related

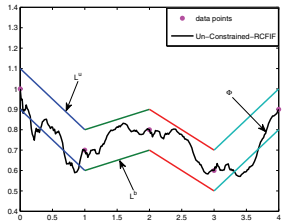

(a) Unconstrained RCFIF Φ_1

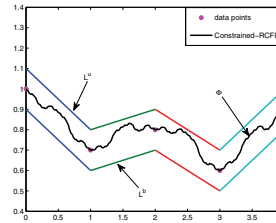

(b) Constrained RCFIF Φ_2

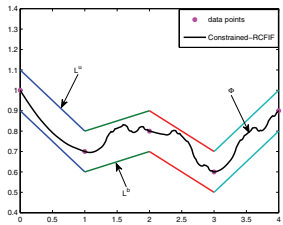

(c) Constrained RCFIF Φ_3, effects of α_1

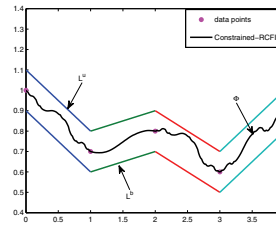

(d) Constrained RCFIF Φ_4, effects of α_2

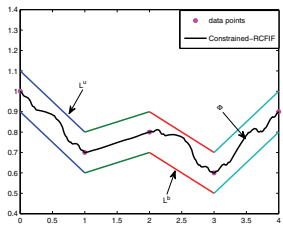

(e) Constrained RCFIF Φ_5, effects of w_2 on Φ_4

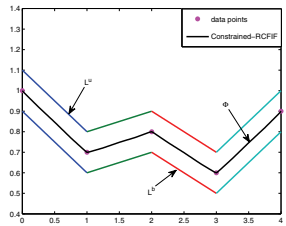

(f) Constrained RCFIF Φ_6, effects of smaller $\alpha_i, w_i, i = 1, 2, 3, 4$

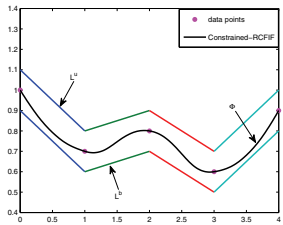

(g) Constrained RCFIF Φ_7, effects of $\alpha_i, w_i, i = 1, 2, 3, 4$

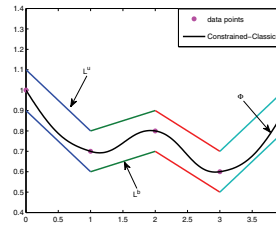

(h) Constrained classical interpolant S

FIGURE 1. $\mathcal{C}^1$-RCFIFs with respect to the IFS parameters in TABLE 1.

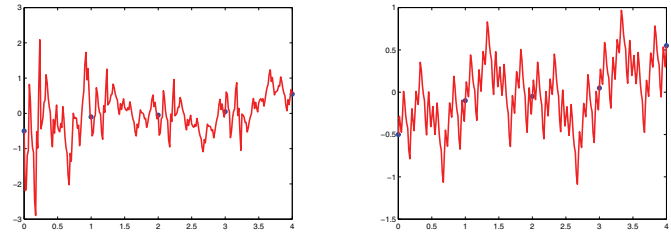

(a) Φ'_1 (b) Φ'_2

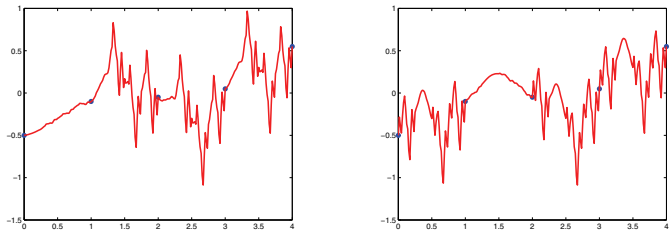

(c) Φ'_3 (d) Φ'_4

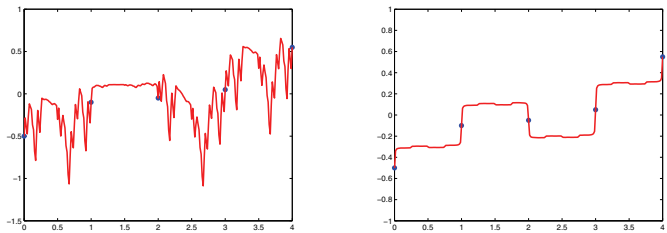

(e) Φ'_5 (f) Φ'_6

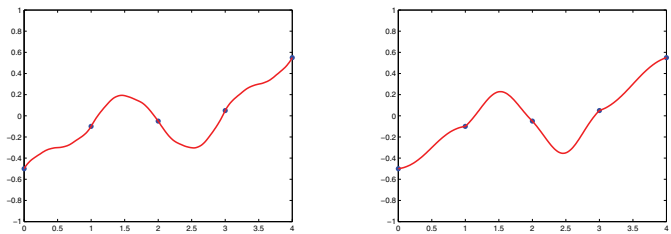

(g) Φ'_7 (h) S'

FIGURE 2. First order partial derivatives of various RCFIFs.

with map L_1 in the given domain. Next, we modify only α_2 with respect to IFS parameters of Φ_2 to generate Φ_4. The perturbation effects of scaling parameter(s) on the shape of Φ_4 are to be noted in comparison with the shape of Φ_3 (Φ_2). By changing the shape parameter w_2 with respect to the IFS parameters of Φ_4, we have constructed the constrained RCFIF Φ_5 in Figure 1(e). For the large value of the shape parameter w_2, the RCFIF Φ_4 converges to a straight line in the second subinterval $[x_2, x_3]$. Similarly, the shape parameters w_i and scaling factors α_i, $i = 1, 2, 3, 4$, are modified in Φ_2 to generate the RCFIF Φ_6 in Figure 1(f), where the RCFIF is similar to a piecewise straight line. It is verified that, for large values of the shape parameters and smaller values of the scaling factors, the RCFIF becomes a piecewise straight line in the given domain. Figure 1(g) represents the graph of Φ_7 and is the smooth curve representation of the RCFIF Φ_2 with the perturbation of all IFS parameters. Finally, by setting all of the scaling factors to zero, we have generated the graph of classical rational cubic interpolant S in Figure 1(h). The optimal values of the IFS parameters for a given original function can be obtained by using a suitable optimization method and the collage theorem [**6**].

From (2.5) and (3.2), the first order partial derivative of the RCFIF interpolates the data $\{(0, -0.5), (1, -0.1), (2, -0.5), (3, 0.05), (4, 0.55\}$. The graphs of the derivative functions of the various rational cubic FIFs $\Phi_1 - \Phi_7$ and the classical rational cubic interpolant S are given in Figures 2(a)–2(h), respectively. Fractality associated with the RCFIFs is evident from Figures 2(a)–2(g), whereas Figure 2(h) indicates that the classical interpolant is piecewise differentiable and smooth. Fractality in the derivative of RCFIFs can be controlled by setting the associated scaling factors to zero in the desired subintervals.

We have estimated the values of the uniform norms of error between the RCFIFs 2(c)–2(g) and the standard RCFIF Figure 2(b) (as the original function) and their derivatives in Table 2. RCFIF Φ_4 is the best uniform approximant for the original function Φ_2, whereas RCFIF Φ_5 is the best C^1-approximant for Φ_2 per the error estimation in Table 2. We believe that flexibility in the choice of the interpolant and fractality in the first derivative of the interpolant inherent with the proposed scheme can be exploited in some nonlinear and non-equilibrium phenomena [**16, 26**]. Fractality in the derivative may be quantified in terms of the box counting dimension or the Hausdorff

TABLE 2. Upper bounds of the error estimates for the various RCFIFs and differentiable RCFIFs.

Error	Upper bound	Error	Upper bound
$\|\Phi_2 - \Phi_3\|_\infty$	0.096382	$\|\Phi_2' - \Phi_3'\|_\infty$	0.827524
$\|\Phi_2 - \Phi_4\|_\infty$	0.072142	$\|\Phi_2' - \Phi_4'\|_\infty$	0.783338
$\|\Phi_2 - \Phi_5\|_\infty$	0.073654	$\|\Phi_2' - \Phi_5'\|_\infty$	0.721856
$\|\Phi_2 - \Phi_6\|_\infty$	0.085490	$\|\Phi_2' - \Phi_6'\|_\infty$	0.876281
$\|\Phi_2 - \Phi_7\|_\infty$	0.088897	$\|\Phi_2' - \Phi_7'\|_\infty$	0.824051
$\|\Phi_2 - S\|_\infty$	0.111313	$\|\Phi_2' - S'\|_\infty$	0.887853

dimension, and this number can be used as an index for the complexity of the underlying phenomenon.

6. Data locality of RCFIFs. In this section, we study the data locality of developed RCFIFs with a small perturbation in interpolation data. Data locality is the property that measures the effect of small local change in the positioning of one data point at a distance along the interpolant.

For simplicity, let us denote a data set, obtained by perturbation in x_3, and obtained by a small change in y_4 as

$$\mathcal{P} := \{(0,1),(1,0.7),(2,0.8),(3,0.6),(4,0.9)\},$$
$$\mathcal{P}_x := \{(0,1),(1,0.7),(\mathbf{2.1},0.8),(3,0.6),(4,0.9)\}$$

and

$$\mathcal{P}_y := \{(0,1),(1,0.7),(2,0.8),(3,\mathbf{0.7}),(4,0.9)\},$$

respectively. We also denote the positive real vectors α, u, v, w, α_x, u_x, v_x, w_x and α_y, u_y, v_y, w_y as IFS parameters corresponding to the standard and perturbed RCFIFs obtained from the data sets $\mathcal{P}$, $\mathcal{P}_x$ and $\mathcal{P}_y$, respectively. We fix the corresponding shape parameters involved in the construction of RCFIF as $u = u_x = u_y = 0.1$ and $v = v_x = v_y = 0.2$.

Now, consider the standard RCFIF Figure 2(a) as the original function Φ_8 with respect to the data set $\mathcal{P}$. The IFS parameters of Figure 3 are detailed in Table 3. We make a change in the x-coordinate x_3 by $\epsilon_x = 0.1$, which gives a new data set $\mathcal{P}_x$. Then, the values

of RCFIF Φ_8 change only in the intervals $[1,2]$ and $[2,3]$ that share the partition point in traditional interpolation techniques like Hermite interpolation. Figures 3(a), 3(c) and 3(e) show the data locality in x-coordinate (x_3) of Φ_8, Φ_9 and the corresponding classical counterpart S, respectively, and they are denoted by $\Phi_{8,x_3+\epsilon_x}$, $\Phi_{9,x_3+\epsilon_x}$ and $S_{x_3+\epsilon_x}$.

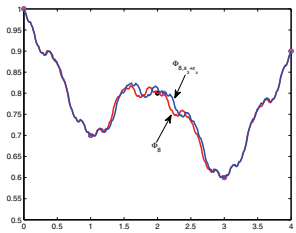

(a) Local change in x_3, Φ_8, $\Phi_{8,x_3+\epsilon_x}$

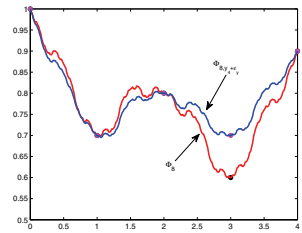

(b) Local change in y_4, Φ_8, $\Phi_{8,y_4+\epsilon_y}$

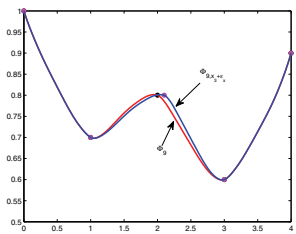

(c) Local change in x_3, Φ_9, $\Phi_{9,x_3+\epsilon_x}$

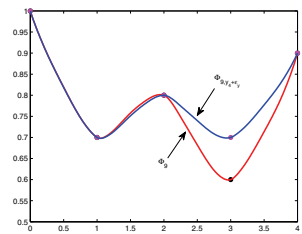

(d) Local change in y_4, Φ_9, $\Phi_{9,y_4+\epsilon_y}$

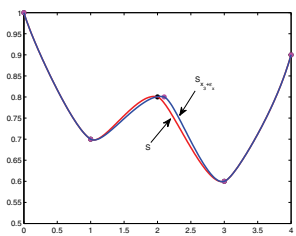

(e) Local change in x_3, S, $S_{x_3+\epsilon_x}$

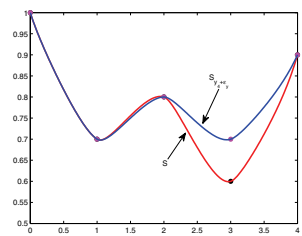

(f) Local change in y_4, S, $S_{y_4+\epsilon_y}$

FIGURE 3. Data locality with respect to the perturbations in x, y coordinates and IFS parameters.

TABLE 3. Corresponding IFS parameters used for RCFIFs in Figure 3.

Figure	Interpolants	IFS parameters
Fig. 3(a)	$\Phi_8, \Phi_{2,x_3+\epsilon_x}$	$\alpha = (0.24, 0.24, 0.24, 0.24)$, $\alpha_x = (0.24, 0.265, 0.215, 0.24)$, $w = (0.5663, 0.5637, 0.5637, 0.5701) = w_x$
Fig. 3(b)	$\Phi_8, \Phi_{2,y_4+\epsilon_y}$	$\alpha = (0.24, 0.24, 0.24, 0.24) = \alpha_y$ $w = (0.5633, 0.5637, 0.5637, 0.5701)$, $w_y = (0.6122, 0.5753, 0.5732, 0.6822)$
Fig. 3(c)	$\Phi_9, \Phi_{2,x_3+\epsilon_x}$	$\alpha = (0.01, 0.01, 0.01, 0.01) = \alpha_x$ $w = (0.6122, 0.5753, 0.5732, 0.6822) = w_x$
Fig. 3(d)	$\Phi_9, \Phi_{7,y_4+\epsilon_y}$	$\alpha = (0.01, 0.01, 0.01, 0.01) = \alpha_y$ $w = (0.6122, 0.5753, 0.5732, 0.6822)$, $w_y = (0.6122, 0.5753, 0.5741, 0.6381)$
Fig. 3(e)	$S, S_{x_3+\epsilon_x}$	$\alpha = (0, 0, 0, 0) = \alpha_x$ $w = (0.6137, 0.5780, 0.5804, 0.6859) = w_x$
Fig. 3(f)	$S, S_{y_4+\epsilon_y}$	$\alpha = (0, 0, 0, 0) = \alpha_y$ $w = (0.6137, 0.5780, 0.5804, 0.6859)$, $w_y = (0.6137, 0.5780, 0.5780, 0.6415)$

We conclude that data locality in a perturbation with respect to the independent variable x is restricted only to the immediate adjacent subintervals of perturbed x-values. Since an RCFIF is implicitly defined, the change in y-coordinate affects the values of the interpolant in the entire domain. We make a change in the y-coordinate y_4 by $\epsilon_y = 0.1$, which gives a new data set $\mathcal{P}_y$. Then, the values of RCFIF Φ_8 change in the domain $[0, 4]$ of the interpolant. Figures 3(b), 3(d) and 3(f) show the data locality in y-coordinate (y_4) of Φ_8, Φ_9 and the corresponding classical counterpart S, respectively, and they are denoted by $\Phi_{8,y_4+\epsilon_y}$, $\Phi_{9,y_4+\epsilon_y}$ and $S_{y_4+\epsilon_y}$. We conclude that data locality in a perturbation with respect to the dependent variable y is spread over the subintervals where the scaling factors are not too small, see Figure 3(b); however, it definitely occurs in the immediate adjacent subintervals of perturbed y-values, see Figures 3(d) and 3(f), irrespective of the magnitude of scaling factors.

7. Conclusions. In this paper, we have constructed $\mathcal{C}^1$-RCFIFs to preserve the constrained aspect of given data. The RCFIF reduces to the traditional rational cubic interpolant by setting all scaling

factors to zero. The RCFIF thus developed converges uniformly to the data generating original function as $h \to 0$, and additionally, if $|\alpha_i| < a_i^3$, then the order of convergence is $O(h^3)$. We have developed the sufficient data-dependent conditions on the rational IFS parameters to preserve the shape of the given data in such a way that the RCFIF lies between two piecewise straight lines. Out of the three shape parameters, the two shape parameters (u_i, v_i) may be used as desired, and the remaining shape parameters and scaling factors can be used for interactive smooth curve design. The affects of the rational IFS parameters on the shape of the RCFIFs are illustrated with respect to the modified IFS parameters. Data locality of the proposed RCFIFs with respect to both independent and dependent parameters were also investigated. The RCFIF developed herein can be used for the visualization of data with or without slopes at the knots. In particular, the proposed method should be an ideal tool in shape-preserving interpolation problems where the data set originates from a constrained data interpolating function $\Phi \in \mathcal{C}^1$, although its derivative is a continuous and nowhere differentiable function. Applications of the proposed RCFIF in geometric modeling problems are under investigation.

Acknowledgments. The first author is thankful to the Department of Science & Technology, India. The authors are thankful to the anonymous referee for extensive comments and constructive criticism that improved the presentation of the paper.

REFERENCES

1. M. Abbas, E. Jamal and J.Md. Ali, *Shape preserving constrained data visualization using spline functions*, Inter. J. Appl. Math. Stat. **29** (2012), 34–50.

2. M. Abbas, A.A. Majid, M.N.H. Awang and J.Md. Ali, *Local convexity shape preserving data visualization by spline function*, ISRN Math. Anal. **2012**, article ID 174048, 1–14.

3. M.R. Asim and K.W. Brodlie, *Curve drawing subject to positivity and more general constraints*, Comp. Graphics **27** (2003), 469–485.

4. M.N.H. Awang, M. Abbas, A.A. Majid and J.Md. Ali, *Data visualization for constrained data using $\mathcal{C}^2$ rational cubic spline*, Proc. World Congr. Eng. Comp. Sci. **1** (2013), 80–85.

5. M.F. Barnsley, *Fractal functions and interpolation*, Constr. Approx. **2** (1986), 303–329.

6. ———, *Fractals everywhere*, Dover Publications, New York, 2012.

7. M.F. Barnsley, J. Elton, D. Hardin and P. Massopust, *Hidden variable fractal interpolation functions*, SIAM J. Math. Anal. **20** (1989), 1218–1242.

8. M.F. Barnsley and A.N. Harrington, *The calculus of fractal interpolation functions*, J. Approx. Th. **57** (1989), 14–34.

9. K.W. Brodlie and S. Butt, *Preserving positivity using piecewise cubic interpolation*, Comp. Graphics **17** (1993), 55–64.

10. A.K.B. Chand and G.P. Kapoor, *Generalized cubic spline fractal interpolation functions*, SIAM J. Numer. Anal. **44** (2006), 655–676.

11. ———, *Spline coalescence hidden variable fractal interpolation functions*, J. Appl. Math **2006** (2006), article ID 36829.

12. A.K.B. Chand and M.A. Navascués, *Generalized Hermite fractal interpolation*, Rev. Roum. Acad. Cienc. Zaragoza **64** (2009), 107–120.

13. A.K.B. Chand, N. Vijender and M.A. Navascués, *Shape preservation of scientific data through rational fractal splines*, Calcolo **51** (2014), 329–362.

14. A.K.B. Chand and P. Viswanathan, *Cubic Hermite and cubic spline fractal interpolation functions*, AIP Conf. Proc. **1479** (2012), 1467–1470.

15. ———, *A constructive approach to cubic Hermite fractal interpolation function and its constrained aspects*, BIT Numer. Math. **53** (2013), 841–865.

16. F.L. Chernousko, I.M. Ananievski and S.A. Reshmin, *Control of nonlinear dynamical systems*: *Methods and applications*, Springer-Verlag, Berlin, 2008.

17. L. Dalla and V. Drakapoulos, *On the parameter identification problem in the plane and polar fractal interpolation functions*, J. Approx. Th. **101** (1999), 289–302.

18. Q. Duan, L. Wang and E.H. Twizell, *A new $\mathcal{C}^2$ rational interpolation based on function values and constrained control of the interpolant curves*, J. Appl. Math. Comp. **61** (2005), 311–322.

19. Q. Duan, G. Xu, A. Liu, X. Wang and F. Cheng, *Constrained interpolation using rational cubic spline with linear denominators*, Korean J. Comp. Appl. Math. **6** (1999), 203–215.

20. F.N. Fritsch and J. Butland, *A method for constructing local monotone piecewise cubic interpolants*, SIAM J. Sci. Stat. Comp. **5** (1984), 303-304.

21. S. Gibert and P.R. Massopust, *The exact Hausdorff dimension for a class of fractal functions*, J. Math. Anal. Appl. **168** (1992), 171–183.

22. J.A. Gregory and R. Delbourgo, *Shape preserving piecewise rational interpolation*, SIAM J. Stat. Comp. **6** (1985), 967–976.

23. J.A. Gregory and M. Sarfraz, *A rational spline with tension*, CAGD **7** (1990), 1–13.

24. D. Halliday, R. Resnick and J. Walker, *Fundamentals of physics*, Wiley, New York, 2010.

25. M.Z. Hussian, M. Sarfraz and M. Hussain, *Scientific data visualization with shape preserving $\mathcal{C}^1$-rational cubic interpolation*, Europ. J. Pure Appl. Math. **3** (2010), 194–212.

26. A. Jayaraman and A. Belmonte, *Oscillations of a solid sphere falling through a wormlike micellar fluid*, Phys. Rev. **67** (2003), 65301.

27. P.D. Massopust, *Interpolation and approximation with splines and fractals*, Oxford University Press, Oxford, 2010.

28. P.R. Massopust, *Fractal functions, fractal surfaces, and wavelets*, Academic Press, Cambridge, MA, 2016.

29. M.A. Navascués and M.V. Sebastian, *Smooth fractal interpolation*, J. Inequal. Appl. **2006** (2006), article ID 78734.

30. M. Sarfraz, M. Al-Mulhem and F. Ashraf, *Preserving monotonic shape of the data using piecewise rational cubic functions*, Comp. Graphics **21** (1997), 5–14.

31. M. Sarfraz and M.Z. Hussian, *Data visualization using rational spline interpolation*, J. Comp. Appl. Math. **189** (2006), 513–525.

32. J.W. Schimdt and W. Heß, *Positivity of cubic polynomials on intervals and positive spline interpolation*, BIT Numer. Math. **28** (1988), 340–352.

33. S.S. Tahira, M. Sarfraz and M.Z. Hussian, *Shape preserving constrained data visualization using rational functions*, J. Prime Res. Math. **7** (2011), 35–51.

34. P. Viswanathan and A.K.B. Chand, *A C^1-rational cubic fractal interpolation function: Convergence and associated parameter identification problem*, Acta. Appl. Math. **136** (2015), 19–41.

35. P. Viswanathan, A.K.B. Chand and M.A. Navascués, *Fractal perturbation preserving fundamental shapes: Bounds on the scale factors*, J. Math. Anal. Appl. **419** (2014), 804–817.

Indian Institute of Technology Madras, Department of Mathematics, Chennai, 600036 India
Email address: **chand@iitm.ac.in**

Indian Institute of Technology Madras, Department of Mathematics, Chennai, 600036 India
Email address: **kurmaths86@gmail.com**